

Quantum Nondecimated Wavelet Transform: Theory, Circuits, and Applications

Brani Vidakovic
Texas A&M University

December 29, 2025

Abstract

The nondecimated or translation-invariant wavelet transform (NDWT) is a central tool in classical multiscale signal analysis, valued for its stability, redundancy, and shift invariance. This paper develops two complementary quantum formulations of the NDWT that embed these classical properties coherently into quantum computation. The first formulation is based on the epsilon-decimated interpretation of the NDWT and realizes all circularly shifted wavelet transforms simultaneously by promoting the shift index to a quantum register and applying controlled circular shifts followed by a wavelet analysis unitary. The resulting construction yields an explicit, fully unitary quantum representation of redundant wavelet coefficients and supports coherent postprocessing, including quantum shrinkage via ancilla-driven completely positive trace preserving maps. The second formulation is based on the Hadamard test and uses diagonal phase operators to probe scale-shift wavelet structure through interference, providing direct access to shift-invariant energy scalograms and multiscale spectra without explicit coefficient reconstruction. Together, these two approaches demonstrate that redundancy and translation invariance can be exploited rather than avoided in the quantum setting. Applications to denoising, feature extraction, and spectral scaling illustrate how quantum NDWTs provide a flexible and physically meaningful foundation for multiscale quantum signal processing.

Keywords: Quantum wavelet transforms, Quantum nondecimated wavelet transform, Epsilon decimation and controlled shifts, Hadamard test and phase encoding, Quantum wavelet shrinkage and CPTP channels, Quantum signal processing

1 Introduction

The nondecimated wavelet transform (NDWT), also known as the stationary or translation-invariant wavelet transform, is one of the most robust multiscale representations in classical signal analysis. In contrast with the standard discrete wavelet transform (DWT), the NDWT avoids dyadic downsampling and instead computes wavelet coefficients at every circular shift and at every resolution level. The resulting representation is redundant but highly stable: small translations of the input signal lead to smooth, predictable changes in the coefficient arrays. Because of this stability, the NDWT has become a standard tool in denoising, spectral estimation, feature extraction, and the analysis of scaling and fractal behavior (Nason & Silverman, 1995; Vidakovic, 1999).

A useful structural interpretation of the NDWT views it as a structured collection of ordinary orthogonal DWTs applied to circularly shifted versions of the signal. For a signal of length $N = 2^n$, the NDWT can be organized into families of 2^j shifted DWTs at each resolution level j . Each individual DWT in this collection is an orthogonal transform and therefore preserves energy. The redundancy of the NDWT arises solely from the inclusion of all shifts, not from any loss of orthogonality. This epsilon-decimated viewpoint, formalized by Nason and Silverman, plays a central role in understanding translation-invariant wavelet analysis and provides a natural bridge to quantum implementations.

This structural property is particularly significant in the quantum setting. Quantum evolution is inherently unitary, and linear transforms that decompose into orthogonal components admit natural realizations as quantum circuits. Since each shifted DWT is orthogonal, the epsilon-decimated family underlying the NDWT can be embedded coherently into a larger Hilbert space, with the shift index promoted to a quantum register. All shifted transforms can then be applied in parallel through quantum superposition. While the classical NDWT itself is not unitary, its epsilon-decimated lift admits a unitary realization that preserves the full redundant multiscale structure.

The purpose of this paper is to develop a systematic and self-contained account of how nondecimated wavelet ideas can be implemented on a quantum computer. Two complementary quantum formulations are presented. The first is based on the epsilon-decimated representation of the NDWT and uses a shift register, controlled circular shifts, and orthogonal wavelet unitaries to generate all shifted wavelet transforms coherently within a single circuit. This construction yields an explicit quantum representation of the redundant coefficient structure and supports subsequent quantum processing, including attenuation and shrinkage via ancilla-driven completely positive trace preserving (CPTP) maps. The second formulation is based on the Hadamard test and diagonal phase operators, and is designed to estimate shift-invariant energy summaries and scalograms directly as quantum expectation values, without explicitly constructing the full redundant coefficient array.

The paper is organized as follows. Section 2 reviews the classical NDWT from the epsilon-decimated perspective, emphasizing its decomposition into orthogonal shifted DWTs. Section 3 introduces the quantum epsilon-decimated NDWT. An amplitude-encoded signal occupies a register of n qubits, while a shift register of L ancilla qubits indexes the required circular shifts, where L denotes the depth of the wavelet transform. Controlled shifts followed by a wavelet unitary realize individual epsilon-decimated branches, and preparation of the ancilla register in a uniform superposition produces the entire family of shifted transforms coherently. Section 4 discusses measurement strategies and the extraction of coefficients, energies, and translation-invariant summaries from the resulting quantum state.

Section 5 presents an alternative quantum formulation of the NDWT based on the Hadamard test. In this approach, each nondecimated wavelet at scale j and shift k is encoded as a diagonal phase unitary. Interference between the signal state and this phase modulation yields local energy contributions as expectation values, producing a redundant scalogram without constructing large nonunitary operators. This formulation is particularly attractive for near-term devices and for applications focused on spectral or scaling behavior rather than explicit coefficient recovery. Subsequent sections address circuit complexity and resource scaling, illustrate applications to denoising and multiscale spectral analysis, and conclude with a discussion of future directions.

Finally, we briefly situate this work within the broader literature on quantum wavelet transforms. Early contributions by Klappenecker (Klappenecker, 1999) and by Fijany and Williams (Fijany & Williams, 1998a, 1998b) demonstrated that orthogonal wavelet transforms can be implemented using quantum circuits composed of local rotations. Later developments extended these ideas to multidimensional transforms, wavelet packets, and efficient synthesis methods (Bagherimehrab & Aspuru-Guzik, 2023; H.-S. Li et al., 2019; Z. H. Li, Li, Li, & Xu, 2018), as well as to related constructions such as quantum wave atom transforms (Podzorova, 2025). These works focus primarily on critically sampled, orthogonal wavelet families. The nondecimated transform considered here belongs to a different category: it is redundant, yet composed entirely of orthogonal components, and is therefore particularly well suited for quantum superposition. The present paper complements existing results by showing that translation-invariant wavelet analysis is not only compatible with quantum computation, but can be implemented coherently and efficiently within a unified quantum framework.

Several Jupyter notebooks featuring `qiskit 2.x` (Abraham, Akhalwaya, Banerjee, Baiardi, et al., 2023) implementations of the quantum NDWT are publicly available at github.com/BraniV/QNDWT. The numerical examples presented in this paper are based on those notebooks.

2 Classical NDWT and the Epsilon Decimation Viewpoint

The classical nondecimated or stationary wavelet transform (NDWT) is a redundant version of the discrete wavelet transform (DWT). Unlike the standard DWT, the NDWT eliminates dyadic downsampling and produces coefficient sequences of the same length as the signal at every resolution level. Because no decimation is performed, the resulting representation is translation invariant: circular shifts of the input signal lead to corresponding shifts of the coefficient arrays without substantial structural change. This property makes the NDWT particularly effective for denoising, spectral estimation, and the analysis of scale dependent phenomena.

Historically, nondecimated wavelet constructions appear early in the wavelet literature. Holschneider and collaborators (Holschneider, Kronland-Martinet, Morlet, & Tchamitchian, 1989) introduced an undecimated filtering scheme that later became widely used in astronomy under the name *a trous* transform (Starck & Murtagh, 1994). Shensa (Shensa, 1992) established a precise connection between the *a trous* algorithm and the Mallat multiresolution scheme, showing that the nondecimated transform can be obtained by executing the standard filter bank without downsampling at any scale. In statistics, Nason and Silverman formalized this construction as the stationary wavelet transform (Nason & Silverman, 1995), while in time series analysis Percival and Walden introduced the maximal overlap DWT (MODWT), a closely related redundant transform with convenient energy normalization (Percival & Walden, 2000).

Let y be a real-valued signal of dyadic length $N = 2^n$, and let W denote the corresponding $N \times N$ orthogonal discrete wavelet transform matrix with L multiresolution levels. The ordinary decimated DWT produces the coefficient vector

$$w = Wy,$$

where the dyadic downsampling inherent in W leads to the well-known lack of translation invariance. To avoid notational conflicts, we use distinct symbols for different wavelet transforms. For standard orthogonal wavelet transforms, detail and scaling (smooth) coefficients are denoted by w and s , respectively. For the nondecimated wavelet transform, we instead use the conventional notation d and a .

A viewpoint that is particularly useful for quantum implementation expresses the NDWT as a structured family of ordinary DWTs applied to circularly shifted versions of the input signal. Let S^ε denote the circular shift operator by ε samples, acting on y via

$$(S^\varepsilon y)[k] = y[(k - \varepsilon) \bmod N].$$

Here S^ε is written in the usual passive (index-shifting) convention; the quantum construction in Section 3 adopts an active convention that differs only by a sign and does not affect orthogonality or the NDWT structure. Define

$$W^{(\varepsilon)} = WS^\varepsilon.$$

Since both W and S^ε are orthogonal, each matrix $W^{(\varepsilon)}$ is itself orthogonal.

If the wavelet transform has depth L , then only the shifts

$$\varepsilon = 0, 1, \dots, 2^L - 1$$

are required. This yields the *epsilon-decimated family*

$$\left\{ W^{(\varepsilon)} y \right\}_{\varepsilon=0}^{2^L-1},$$

a collection of 2^L ordinary wavelet transforms, each producing N coefficients. The total number of coefficients in this family is therefore $N2^L$.

The classical NDWT consists of $(L+1)N$ coefficients: N detail coefficients at each resolution level $j = 1, \dots, L$ and N scaling coefficients at the coarsest level. These coefficients are obtained from the epsilon-decimated family through a deterministic alignment and interleaving procedure. At resolution level j , each wavelet filter admits 2^j distinct circular shifts. The stationary transform retains exactly one coefficient per spatial location, corresponding to the appropriate equivalence class of shifts modulo 2^j .

This selection has a fixed linear structure. There exists a matrix P , depending only on N and L , such that

$$\text{NDWT}(y) = P \left(\left\{ W^{(\varepsilon)} y \right\}_{\varepsilon=0}^{2^L-1} \right),$$

where P extracts exactly $(L+1)N$ coefficients from the full epsilon-decimated collection and reorders them into the standard stationary wavelet form.

The epsilon-decimation viewpoint therefore expresses the classical NDWT as a union of orthogonal components followed by a structured linear projection that enforces translation invariance. This formulation is especially convenient in the quantum setting. Each operator $W^{(\varepsilon)}$ is orthogonal and thus admits a unitary realization, and quantum mechanics naturally allows coherent superpositions over the shift index ε . In the next section, we exploit this characterization to construct a quantum operator that applies all $W^{(\varepsilon)}$ coherently within a single circuit.

3 Quantum Epsilon Decimation and NDWT Operator

We now promote the classical epsilon-decimated representation of the NDWT to a quantum operator. The construction proceeds in three steps: (i) introduce a shift register prepared in superposition, (ii) perform a controlled circular shift on the data register, and (iii) apply a wavelet analysis unitary. Together, these operations yield a coherent quantum realization of the full epsilon-decimated family of wavelet transforms.

Throughout this section, operators are interpreted from context. Linear operators acting on classical vectors and their quantum counterparts are denoted by the same symbols, with the distinction between matrices and unitaries determined by whether they act on vectors or on quantum registers.

For a discrete signal of length $N = 2^n$, the data register consists of n qubits and encodes the normalized signal as an amplitude-encoded state $|y\rangle$. In examples, we sometimes denote the unnormalized data by x , with $y = x/\|x\|$ the normalized version used to prepare the amplitude-encoded state $|y\rangle$.

An NDWT of depth L requires 2^L circular shifts. We therefore introduce an ancilla register of L qubits carrying a shift index

$$|\varepsilon\rangle, \quad \varepsilon \in \{0, 1, \dots, 2^L - 1\},$$

so that the joint Hilbert space has dimension $2^L N$.

Controlled circular shifts. The circular shift operator acts on computational basis states as

$$S^\varepsilon |k\rangle = |(k + \varepsilon) \bmod N\rangle. \quad (1)$$

Conditioning this operation on the ancilla register yields the controlled shift operator

$$U_{\text{shift}} = \sum_{\varepsilon=0}^{2^L-1} |\varepsilon\rangle\langle\varepsilon| \otimes S^\varepsilon. \quad (2)$$

In (1) we adopted the active convention for the quantum shift, which differs from the classical indexing in Section 2 by a sign convention only and does not affect orthogonality or the NDWT structure.

A common wavelet analysis unitary acting on all branches. Let W denote the orthogonal discrete wavelet transform corresponding to a chosen wavelet family. Its quantum implementation is a unitary acting on the data register. Its application is

defined by

$$U_{\text{wavelet}} = \sum_{\varepsilon=0}^{2^L-1} |\varepsilon\rangle\langle\varepsilon| \otimes W = I \otimes W, \quad (3)$$

so that the same wavelet analysis block is applied on every branch of the superposition.

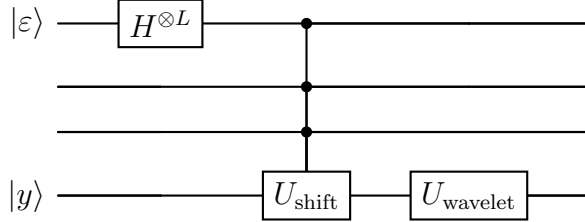


Fig. 1: Quantum epsilon-decimation architecture. An L -qubit ancilla register is placed in a uniform superposition by $H^{\otimes L}$. Conditioned on ε , the data register undergoes S^ε followed by the wavelet analysis unitary W . Each coherent branch implements one epsilon-decimated wavelet transform.

Quantum epsilon-decimated NDWT. Combining the controlled shift and controlled wavelet operators gives

$$U_{\text{NDWT}} = U_{\text{wavelet}} U_{\text{shift}} = \sum_{\varepsilon=0}^{2^L-1} |\varepsilon\rangle\langle\varepsilon| \otimes WS^\varepsilon, \quad (4)$$

so that each branch ε carries the shifted wavelet transform WS^ε .

If the ancilla register is prepared in the uniform superposition

$$|\Xi\rangle = \frac{1}{\sqrt{2^L}} \sum_{\varepsilon=0}^{2^L-1} |\varepsilon\rangle,$$

then the joint action of U_{NDWT} yields

$$U_{\text{NDWT}}(|\Xi\rangle \otimes |y\rangle) = \frac{1}{\sqrt{2^L}} \sum_{\varepsilon=0}^{2^L-1} |\varepsilon\rangle \otimes WS^\varepsilon |y\rangle. \quad (5)$$

Each branch of the superposition corresponds to one element of the classical epsilon-decimated library, now realized coherently.

For a fixed shift state $|\varepsilon\rangle$,

$$U_{\text{NDWT}}(|\varepsilon\rangle \otimes |y\rangle) = |\varepsilon\rangle \otimes WS^\varepsilon |y\rangle,$$

and the superposed form in (5) follows by linearity. Since the operators WS^ε act on

mutually orthogonal ancilla sectors, the overall operator U_{NDWT} is unitary. The quantum NDWT thus appears as a block-diagonal unitary conditioned on the shift register.

The circuit depth of the quantum NDWT matches that of the underlying decimated wavelet transform. The data register carries the multilevel wavelet structure, while the ancilla register records redundant shift positions without increasing transform depth.

Example 1. Fully Quantum Two-Level Nondecimated Haar Transform. This example presents a minimal realization of a fully quantum nondecimated Haar wavelet transform of depth 2 for a signal of length $N = 8$, $x = (2, 1, 9, 0, 3, -10, 2, 4)$. The signal is rescaled to $[-1, 1]$ and normalized to prepare the data register

$$|y\rangle = \sum_{k=0}^7 y_k |k\rangle,$$

with

$$y = (0.165567, 0.09934, 0.629153, 0.033113, 0.231793, -0.629153, 0.165567, 0.29802).$$

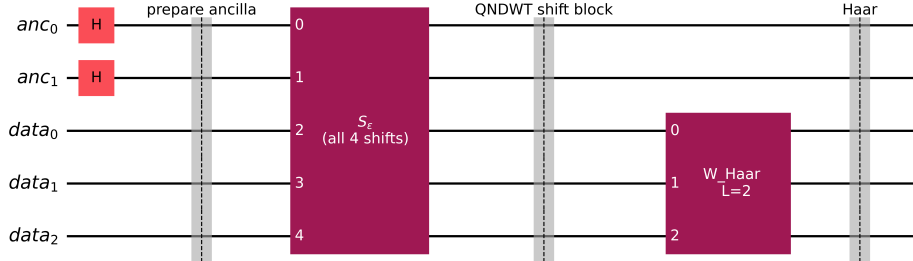


Fig. 2: Fully quantum two-level Haar QNDWT on $N = 8$. The circuit coherently prepares four shifted Haar transforms in superposition.

The transform proceeds as

$$|0\rangle^{\otimes 2} |y\rangle \xrightarrow{H^{\otimes 2}} \frac{1}{2} \sum_{\varepsilon=0}^3 |\varepsilon\rangle |y\rangle \xrightarrow{U_{\text{shift}}} \frac{1}{2} \sum_{\varepsilon=0}^3 |\varepsilon\rangle S^\varepsilon |y\rangle \xrightarrow{W} \frac{1}{2} \sum_{\varepsilon=0}^3 |\varepsilon\rangle W S^\varepsilon |y\rangle. \quad (6)$$

ε	$s_{2,1}$	$s_{2,2}$	$w_{2,1}$	$w_{2,2}$	$w_{1,1}$	$w_{1,2}$	$w_{1,3}$	$w_{1,4}$
0	0.736842	0.052632	-0.315789	-0.684211	0.074432	0.669891	0.967620	-0.148865
1	0.947368	-0.157895	-0.210526	0.578947	0.148865	-0.595458	-0.223297	-0.893188
2	0.578947	0.210526	0.157895	0.842105	-0.148865	0.074432	0.669891	0.967620
3	0.000000	0.789474	-0.736842	0.368421	-0.893188	0.148865	-0.595458	-0.223297

Table 1: Quantum 2-level Haar coefficients per shift.

This example serves as a pedagogical benchmark and a building block for larger QNDWT constructions and subsequent quantum processing of wavelet coefficients. The implementation is available in `QNDWT001.ipynb` in the accompanying `qiskit` repository.

index	1	2	3	4	5	6	7	8
d_1	0.074432	-0.595458	0.669891	-0.223297	0.967620	-0.893188	-0.148865	0.148865
d_2	-0.315789	0.368421	0.842105	0.578947	-0.684211	-0.736842	0.157895	-0.210526
a_2	0.736842	0.789474	0.210526	-0.157895	0.052632	0.000000	0.578947	0.947368

Table 2: NDWT coefficients from fully quantum QNDWT state.

Example 2. Fully Quantum QNDWT for a Doppler Signal. We illustrate the quantum nondecimated Haar wavelet transform (QNDWT) on the Doppler test signal of length $N = 64$ (Fig. 3, left panel). The signal is amplitude encoded in a six qubit data register, and a three qubit ancilla prepares a uniform superposition of eight circular shifts. Each ancilla value controls the corresponding circular shift on the data register, so the circuit coherently prepares all shifted versions of the input.

A three level Haar transform is then applied once to the data register. For every ancilla value, the resulting state contains the Haar coefficients of a different circular shift. From the full statevector we extract, for each shift, the detail vectors $w_1^{(\varepsilon)}, w_2^{(\varepsilon)}, w_3^{(\varepsilon)}$ and the smooth approximation $s_3^{(\varepsilon)}$.

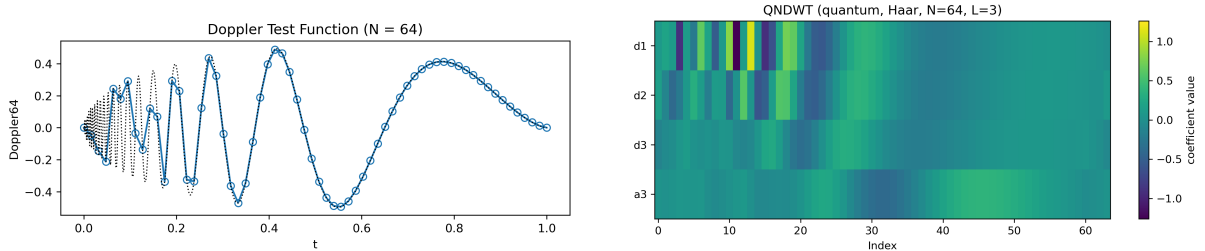


Fig. 3: (Left) Doppler test signal sampled at $N = 64$ equispaced (in t) points. (Right) Quantum Nondecimated Wavelet Transform of depth $L = 3$.

The nondecimated wavelet sequences are assembled by undoing the shifts and aggregating the detail vectors over all ancilla values. This produces the standard NDWT components d_1, d_2, d_3 , and a_3 , each of length 64, as in Fig. 3, right panel.

A stacked plot of these sequences reproduces the classical Haar NDWT of the Doppler signal. This example is implemented in `QNDWT003.ipynb`.

This example demonstrates the shift based realization of the QNDWT. All redundant coefficients are generated coherently in a single circuit, with no measurements required. The next examples introduce the Hadamard test formulation, which provides a complementary measurement based mechanism for estimating wavelet energies and spectra without constructing the full redundant representation.

The next section describes how the joint state in (5) is interrogated to extract coefficients, energies, and translation-invariant summaries.

4 Measurement and Extraction of Information from the Quantum NDWT

The quantum NDWT prepares a coherent superposition of all epsilon-decimated wavelet transforms,

$$|\Psi_{\text{NDWT}}\rangle = \frac{1}{\sqrt{2^L}} \sum_{\varepsilon=0}^{2^L-1} |\varepsilon\rangle \otimes WS^\varepsilon|y\rangle. \quad (7)$$

The data register contains the wavelet coefficients corresponding to a given circular shift, while the ancilla register encodes the shift index ε . This joint structure supports several distinct modes of information extraction, depending on how the ancilla is measured or discarded.

Projective measurement of the ancilla. If the ancilla register is measured in the computational basis, the joint state collapses to one of the decimated transforms

$$|y_\varepsilon\rangle = WS^\varepsilon|y\rangle,$$

each occurring with probability 2^{-L} . Operationally, this corresponds to selecting a single circular shift and performing the usual orthogonal wavelet transform. Although this procedure discards the redundant information, it provides a direct quantum implementation of the classical decimated DWT as a special case of the QNDWT architecture.

Full NDWT coefficient recovery. To reconstruct the full redundant NDWT coefficient table, one may perform conditional measurements of the data register given the ancilla outcome. Repeating this procedure for all values of ε recovers the entire epsilon-decimated library and, after alignment, the $(L+1)N$ stationary coefficients. The required number of measurement passes mirrors the classical cost of enumerating all circular shifts, while the underlying unitary preparation of $|\Psi_{\text{NDWT}}\rangle$ remains fixed and independent of N .

Levelwise energies and translation-invariant summaries. Many applications of the NDWT rely not on individual coefficients but on aggregated quantities such as levelwise energies, norms, or translation-invariant summaries. These quantities are naturally obtained by tracing out the ancilla register. Let

$$\rho = |\Psi_{\text{NDWT}}\rangle\langle\Psi_{\text{NDWT}}|$$

denote the joint density operator, and define the reduced state on the data register by

$$\rho_D = \text{Tr}_A(\rho).$$

This partial trace coherently averages over all circular shifts. Consequently, expectation values of observables acting only on the data register reproduce the same shift-averaged quantities computed by classical NDWT energy estimators. In particular, the energy of detail level j may be estimated by measuring the projector onto the corresponding wavelet subspace.

Cross-scale statistics and correlations. The redundancy of the NDWT is especially valuable when analyzing local oscillatory or self-similar structure. Because all shifts are present simultaneously in $|\Psi_{\text{NDWT}}\rangle$, cross-scale correlations such as

$$\langle d_{j,k} d_{j',k'} \rangle$$

and other multilevel summaries can be estimated from repeated measurements on ρ_D alone, without resolving or enumerating the shift index. In this sense, the quantum representation compresses all 2^L classical transforms into a single object from which rich statistical structure can be extracted at measurement time.

Hybrid measurement strategies. Intermediate strategies are also possible. Partial or weak measurements of the ancilla can preserve coherence among subsets of shifts while reducing estimator variance. Such hybrid procedures have no direct classical analogue and may enable efficient quantum protocols for signal classification, anomaly detection, or denoising based on redundant wavelet representations.

Overall, the quantum NDWT provides a unified mechanism for generating, storing, and interrogating the full redundant family of wavelet representations traditionally obtained through circular shifts. The representation is efficient to prepare, requires no repeated unitary transforms, and supports flexible measurement protocols tailored to the statistical task of interest. These properties make the QNDWT a natural foundation for adaptive quantum signal processing and quantum wavelet-based inference.

Quantum analogue of the NDWT projection. In the classical setting, the NDWT is obtained from the epsilon-decimated library $z(y) \in \mathbb{R}^{N2^L}$ by a fixed linear operator $P : \mathbb{R}^{N2^L} \rightarrow \mathbb{R}^{(L+1)N}$, which selects, aligns, and aggregates coefficients across shifts to form the stationary sequences d_j , $j = 1, \dots, L$, and a_L . Although linear, this projection is not unitary: it reduces dimension, mixes coefficients across epsilon blocks, and performs shift averaging. As such, it cannot be implemented directly as a quantum circuit.

In the quantum construction, shift averaging arises naturally through partial tracing. Tracing out the ancilla register yields the reduced state ρ_D , which plays a role analogous to the classical projection P . In particular, the diagonal entries of ρ_D satisfy

$$(\rho_D)_{k,k} = \frac{1}{2^L} \sum_{\varepsilon=0}^{2^L-1} |(WS^\varepsilon y)_k|^2,$$

which coincides with the local shift-averaged energy used in the stationary wavelet transform. More generally, for any observable O acting only on the data register,

$$\mathrm{Tr}(O\rho_D) = \frac{1}{2^L} \sum_{\varepsilon=0}^{2^L-1} \langle y | (S^\varepsilon)^* W^* O W S^\varepsilon | y \rangle,$$

reproducing the classical translation-invariant NDWT statistics.

In this sense, the classical projection P and the quantum partial trace $\mathrm{Tr}_A(\cdot)$ serve analogous purposes for quadratic summaries and invariant features. The classical NDWT compresses the epsilon-decimated library by explicit linear aggregation, while the quantum NDWT compresses a coherent superposition via a completely positive trace preserving map. Shift invariance thus emerges naturally in the quantum setting as an instance of quantum coarse graining, implemented by partial tracing rather than by a unitary operator.

5 Hadamard Test Nondecimated Wavelet Transform

The classical nondecimated wavelet transform produces a redundant, shift-invariant multiscale representation by applying the same wavelet filter at all circular shifts. Although this transform is nonunitary due to the absence of downsampling, a quantum analogue can be constructed that preserves unitarity by changing the mode of access to wavelet information. Instead of explicitly generating signed wavelet coefficients, the Hadamard test formulation encodes scale-shift wavelets as diagonal phase operators and recovers *energy-based* quantities through interference (Aharonov, Jones, & Landau, 2009). The result is a coherent, fully unitary mechanism for constructing redundant NDWT scalograms without replicating the signal or synthesizing large block-structured operators.

Let the amplitude-encoded signal be

$$|y\rangle = \frac{1}{\|y\|} \sum_{n=0}^{N-1} y_n |n\rangle,$$

and let $\psi_{j,k}[n]$ denote the discrete nondecimated wavelet at scale j and circular shift k . To probe the local wavelet energy associated with (j, k) , define the diagonal phase unitary

$$U_{\phi,j,k} = \mathrm{diag}(e^{i\theta\psi_{j,k}[0]}, e^{i\theta\psi_{j,k}[1]}, \dots, e^{i\theta\psi_{j,k}[N-1]}),$$

where $\theta > 0$ is a tunable phase-gain parameter. Applying a Hadamard test to $U_{\phi,j,k}$

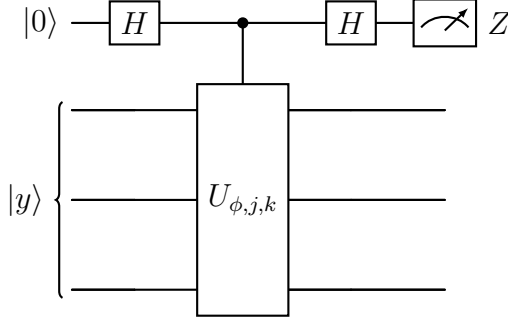


Fig. 4: Hadamard test circuit for a nondecimated wavelet at scale j and shift k . The data register holds the amplitude-encoded signal $|y\rangle$. The ancilla controls the diagonal phase operator $U_{\phi,j,k}$ and is measured in the Z basis to estimate $\mathbb{E}[Z_{j,k}] = \text{Re}\langle y|U_{\phi,j,k}|y\rangle$. To access the imaginary part, an S gate is inserted on the ancilla before the final Hadamard.

yields the expectation value

$$\mathbb{E}[Z_{j,k}] = \text{Re}\langle y|U_{\phi,j,k}|y\rangle = \sum_{n=0}^{N-1} |y_n|^2 \cos(\theta \psi_{j,k}[n]).$$

For sufficiently small θ , the cosine admits a second-order expansion and

$$\mathbb{E}[Z_{j,k}] \approx 1 - \frac{1}{2}\theta^2 \sum_{n=0}^{N-1} |y_n|^2 \psi_{j,k}[n]^2, \quad (8)$$

so that deviations of $\mathbb{E}[Z_{j,k}]$ from 1 encode the *local NDWT energy* at scale j and shift k . The approximation holds provided $\theta \max_n |\psi_{j,k}[n]| \ll 1$, a condition easily satisfied for compactly supported wavelets at fixed resolution.

The Hadamard-test formulation of the NDWT therefore does not produce signed wavelet coefficients. Each query yields a real expectation value of the form (8), which in the small-angle regime equals 1 minus a constant multiple of the quadratic quantity

$$\sum_{n=0}^{N-1} |y_n|^2 \psi_{j,k}[n]^2.$$

As a consequence, the Hadamard NDWT produces a redundant, shift-invariant *energy scalogram*, rather than the $(L+1)N$ coefficient array generated by the epsilon-decimated quantum NDWT. This distinction is fundamental: the Hadamard formulation is ideally suited for tasks based on energies and spectra, such as smoothing, multiscale spectral estimation, and scaling or Hurst exponent analysis—but it does not support coefficientwise shrinkage or direct signal reconstruction.

From a computational perspective, the dominant cost is the controlled application of $U_{\phi,j,k}$. For Haar wavelets, the diagonal entries of $U_{\phi,j,k}$ assume only a small number

of distinct values, and the resulting gate depth scales as $\log N$. For smoother wavelets the filters broaden, but the operator remains diagonal, allowing efficient synthesis via sparse phase-gradient constructions. Each pair (j, k) requires only a single Hadamard test, so the total cost grows linearly with the number of scale-shift locations probed and logarithmically with N .

The parameter θ controls the tradeoff between linearity and sensitivity. Larger values increase signal contrast but reduce the validity of the quadratic approximation, while smaller values improve linearity at the expense of higher shot noise. In practice, values of θ in the range $[10^{-2}, 10^{-1}]$ provide a good compromise. Because the Hadamard measurement outcome is a Bernoulli random variable, the number of shots required to estimate $\mathbb{E}[Z_{j,k}]$ with accuracy ε scales as

$$\text{shots} \sim \varepsilon^{-2}.$$

Aggregated quantities such as levelwise energies or averaged scalograms typically require fewer shots due to variance reduction across shifts.

Noise in the Hadamard NDWT primarily affects the ancilla. Dephasing reduces interference contrast and biases estimates toward zero, but can be mitigated using short-depth phase constructions or echo techniques. Amplitude damping on the data register perturbs the encoded amplitudes, but since the quantities of interest are expectation values of diagonal unitaries, their sensitivity is comparable to other overlap estimation tasks and generally less severe than full state tomography.

The Hadamard NDWT is closely related to the epsilon-decimated quantum NDWT introduced earlier. Both yield redundant, shift-invariant multiscale representations using unitary operations. The epsilon-decimated formulation generates explicit coefficient vectors suitable for further coherent processing, including quantum shrinkage. The Hadamard formulation, by contrast, accesses the same multiscale structure through phase modulation and interference, producing expectation-based energy summaries that are particularly well suited for near-term devices. Together, these two approaches provide complementary quantum realizations of the classical NDWT: one operating in the coefficient domain and the other in the energy domain.

Example 3. QNDWT via the Hadamard Test. This example illustrates how the Hadamard test can be used to probe localized wavelet energies and their relationship to the nondecimated structure of the QNDWT. We consider the Doppler function sampled at $N = 128$ equispaced points. With $L = 3$ resolution levels, the nondecimated Haar transform produces four sequences d_1, d_2, d_3 , and a_3 , each of length 128. These are

assembled into the 4×128 coefficient matrix

$$W_{QNDWT} = \begin{pmatrix} d_1 \\ d_2 \\ d_3 \\ a_3 \end{pmatrix},$$

shown in left panel of Figure 5.

To connect with the Hadamard formulation, consider the orthogonal Haar transform matrix W . Let x denote the Doppler samples and $y = x/\|x\|$ the normalized signal. The decimated coefficients are $w = Wy$, and the energy of coefficient w_k satisfies

$$|w_k|^2 = \frac{1 - \langle y|U_k|y \rangle}{2}, \quad U_k = W^\top(I - 2|k\rangle\langle k|)W.$$

Thus, $|w_k|^2$ can be estimated by a Hadamard test with a single ancilla qubit. In this example, we select a coefficient w_k in the finest detail band of the decimated transform and evaluate $\langle y|U_k|y \rangle$ on a simulator. The Hadamard estimate agrees with the classical energy $|w_k|^2$ up to numerical precision (right panel in Fig. 5).

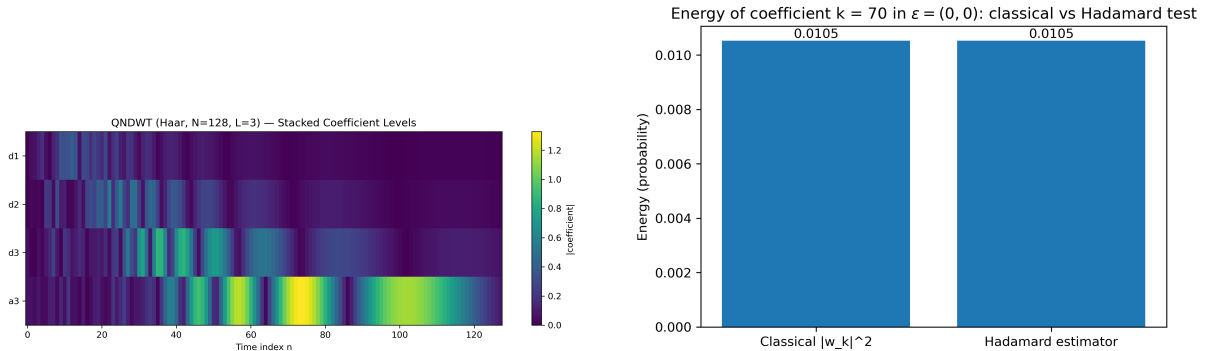


Fig. 5: (Left) W_{QNDWT} of the Doppler function sampled at $N = 128$ equispaced points; (Right) The Hadamard estimate for $|w_k|$ agrees with the classical energy up to numerical precision

Because individual NDWT coefficients can be expressed as finite linear combinations of decimated coefficients across shifts, the Hadamard test provides a quantum mechanism for interrogating localized wavelet energy at specific scales or positions, even when the full QNDWT is generated implicitly or classically. This example is implemented in the notebook `QNDWT004.ipynb` using qiskit 2.x.

6 Circuit Complexity and Resource Scaling of the Quantum NDWT

Sections 3–5 introduced two complementary quantum formulations of the classical NDWT. In the epsilon–decimated approach (Section 3), a single unitary preparation produces the joint state that coherently encodes all shifted wavelet transforms. In the Hadamard approach (Section 5), one probes shift–invariant multiscale information through expectation values, yielding an energy scalogram rather than signed coefficients. This section summarizes the corresponding circuit resources and clarifies how the quantum constructions compare to the classical NDWT cost.

Classically, a straightforward NDWT evaluation can be viewed as applying an orthogonal DWT to many circular shifts of the signal. Relative to one DWT, the redundant transform introduces a substantial overhead in computation and storage because multiple shifted transforms must be generated or emulated. In the quantum setting, redundancy is handled differently: the epsilon–decimated construction represents all shifts coherently in a single state, while the Hadamard construction accesses multiscale energies via repeated but shallow interference experiments.

Epsilon–decimated architecture (state preparation). The unitary in Section 3 has the form

$$U_{\text{NDWT}} = \sum_{\varepsilon=0}^{2^L-1} |\varepsilon\rangle\langle\varepsilon| \otimes WS^\varepsilon,$$

acting on an n –qubit data register and an L –qubit shift register. The dominant coherent primitives are therefore: (i) controlled modular shifts on the data register and (ii) a wavelet analysis unitary W .

A modular addition by ε on $n = \log_2 N$ qubits can be implemented using standard quantum adders with depth $O(n)$ (and often better with hardware–specific optimizations). The wavelet unitary W depends on the chosen wavelet family. For Haar, W admits particularly shallow circuit realizations built from Hadamards and swaps. For compactly supported orthogonal wavelets (Daubechies, Symmlets, etc.), W can be compiled into elementary single–qubit and controlled rotations following standard factorizations of orthogonal filter banks. The key point for resource scaling is that the epsilon–decimated construction applies W *once* to the data register, not 2^L times: the shift index lives in an orthogonal ancilla sector, so redundancy does not introduce additional unitary depth.

The circuit width is $n + L$ qubits in the NDWT setting emphasized here (depth L and 2^L shifts). A fully general “all circular shifts” construction would require n shift qubits, but this generalization is not needed for the NDWT depth parameterization and is best viewed as an optional extension. The controlled structure introduces a constant–factor overhead in gate counts relative to the underlying implementations of S^ε and W .

A practical caveat is that while the full redundant library is prepared coherently, extracting *all* coefficients as classical numbers still requires many measurements (Section 4). The principal advantage of the epsilon-decimated architecture is therefore the availability of the redundant representation as a *quantum object* for subsequent coherent processing (e.g., attenuation or shrinkage via CPTP maps), with measurements postponed and tailored to the downstream task.

Hadamard architecture (energy queries). The Hadamard formulation (Section 5) estimates multiscale energies by applying a controlled diagonal unitary $U_{\phi,j,k}$ and measuring a single ancilla qubit. For each scale-shift pair (j, k) , one Hadamard test requires: (i) one ancilla qubit, (ii) a controlled application of $U_{\phi,j,k}$ (or an equivalent controlled implementation), and (iii) two Hadamard gates plus a projective measurement. The data register preparation of $|y\rangle$ is common to both architectures.

For Haar wavelets, the diagonal phases take only a small set of distinct values, and the depth of $U_{\phi,j,k}$ scales like $O(\log N)$. For smoother wavelets, diagonal synthesis remains efficient because only phase rotations are required; standard decompositions yield gate counts that are polylogarithmic in N for fixed precision. Thus, the unitary depth per local energy estimate is typically $O(\log N)$, while the overall runtime scales linearly with the number of scale-shift locations (j, k) that must be probed.

Shot complexity follows standard overlap-estimation scaling: estimating a single real quantity to accuracy ε requires

$$\text{shots} \sim \varepsilon^{-2},$$

since the Hadamard outcome is Bernoulli. In practice, NDWT summaries such as level energies and averaged scalograms aggregate information across many (j, k) locations and therefore benefit from variance reduction by averaging, often reducing the effective number of shots per location.

Comparison of the two quantum formulations. The epsilon-decimated QNDWT trades additional qubits for a single coherent preparation: the entire redundant library is present in one joint state and can be processed coherently before measurement. This is the appropriate architecture when one requires coefficient-domain operations (e.g., attenuation channels, coefficientwise nonlinearities, or coherent multiscale feature extraction).

The Hadamard formulation minimizes the ancilla footprint and replaces explicit coefficient generation by repeated energy queries. It is therefore especially attractive when the end goal is a shift-invariant energy scalogram, multiscale spectra, or other quadratic summaries, and when near-term constraints favor shallow controlled diagonal operations and measurement-based estimation.

In short, the two constructions serve different use cases: epsilon-decimated QNDWT provides coefficient access for coherent postprocessing, whereas Hadamard QNDWT provides direct access to energy summaries with minimal circuit structure.

Noise, decoherence, and CPTP effects. The relevance of noise depends on which information is being extracted. In the epsilon-decimated representation, decoherence acts through completely positive trace preserving (CPTP) maps on the joint system. Phase damping suppresses off-diagonal terms in the computational basis and therefore reduces coherence among different shift sectors. However, many NDWT-based tasks (e.g., level energies and translation-invariant norms) depend primarily on diagonal entries of the reduced state on the data register. Since phase damping leaves these diagonal entries unchanged, loss of coherence in the ancilla effectively converts quantum superposition into classical averaging over shifts, which is often sufficient for energy-based summaries.

Amplitude damping on the data register perturbs the amplitude encoding and can distort numerical coefficient values. Its effect is therefore more pronounced when the goal is coefficient recovery than when the goal is aggregated quadratic summaries. This aligns with the measurement discussion in Section 4: tasks based on $\rho_D = \text{Tr}_A(\rho)$ are naturally more tolerant to ancilla decoherence than tasks requiring full coefficient readout.

In the Hadamard formulation, the dominant noise mechanism is ancilla dephasing or phase errors in the synthesis of $U_{\phi,j,k}$. These reduce interference visibility and bias estimates toward zero, but the circuits remain shallow and can be combined with echo-style mitigation. Moreover, redundancy in the scalogram supports additional averaging across (j, k) locations.

Finally, noise can also be used constructively as an attenuation mechanism. In the epsilon-decimated setting, controlled dephasing or amplitude damping can implement soft attenuation of high-frequency detail components, providing a physically meaningful route to quantum wavelet shrinkage via CPTP channels. In the Hadamard setting, controlled dephasing of the ancilla or deliberate coarse graining of phase resolution implements analogous attenuation directly at the level of expectation values. These connections motivate the shrinkage and denoising applications developed later.

Overall, both quantum NDWT formulations replace explicit classical enumeration of shifts by either coherent state preparation (epsilon-decimated QNDWT) or by efficient energy queries (Hadamard QNDWT). The resulting resource requirements scale polynomially in $n = \log_2 N$ for fixed wavelet families and fixed precision, and they remain compatible with intermediate-scale quantum devices, especially for tasks focused on translation-invariant multiscale summaries rather than full coefficient readout.

7 Applications of the Quantum NDWT

Sections 3–5 provide two complementary quantum formulations of the classical NDWT. The epsilon-decimated construction of Section 3 prepares a single coherent state encoding all circularly shifted wavelet transforms, enabling coefficient-domain postprocessing prior

to measurement. Section 4 then describes how measurement choices and the reduced state $\rho_D = \text{Tr}_A(\rho)$ support translation-invariant summaries. In contrast, the Hadamard formulation of Section 5 does not aim to output signed coefficients; rather, it accesses scale-shift energies and spectra through expectation values. The applications below are organized accordingly: we first describe coefficientwise operations in the redundant wavelet domain, and then energywise spectral and scaling summaries.

7.1 Coefficientwise processing: Shrinkage via CPTP attenuation

In the epsilon-decimated formulation the quantum NDWT prepares the coherent library

$$|\Psi_{\text{NDWT}}\rangle = U_{\text{NDWT}}(|\Xi\rangle \otimes |y\rangle) = \frac{1}{\sqrt{2^L}} \sum_{\varepsilon=0}^{2^L-1} |\varepsilon\rangle \otimes WS^\varepsilon|y\rangle, \quad (9)$$

where

$$|\Xi\rangle = \frac{1}{\sqrt{2^L}} \sum_{\varepsilon=0}^{2^L-1} |\varepsilon\rangle$$

is the uniform superposition over the 2^L shift indices associated with transform depth L . Classically, translation-invariant denoising applies a shrinkage rule to each shifted transform and then averages across shifts. In the quantum setting, a single preparation of $|\Psi_{\text{NDWT}}\rangle$ makes all shifted coefficient vectors available coherently. One may therefore implement coefficientwise shrinkage as attenuation acting on the data register while leaving the shift register untouched. This yields a quantum analogue of translation-invariant shrinkage without explicitly enumerating or reapplying transforms.

Let ρ denote the density operator of the joint state and let ρ_D be the reduced state on the data register after tracing out the shift register. A diagonal (or approximately diagonal) completely positive trace preserving (CPTP) map acting in the wavelet domain,

$$\rho_D \mapsto \mathcal{E}(\rho_D) = \sum_k E_k \rho_D E_k^*, \quad (10)$$

with Kraus operators that selectively attenuate fine-scale or small-magnitude components, acts as a soft thresholding mechanism. Since the same attenuation is applied uniformly across all shift sectors, the resulting contraction implements a shift-invariant shrinkage rule at the level of the coherent representation.

Phase damping channels provide smooth, scale-dependent attenuation, typically suppressing fine-scale content more strongly than coarse-scale content. Amplitude damping channels permit firm and soft threshold effects by tuning the damping strength. Since the redundant coefficient structure is already present in (9), attenuation acts simultaneously

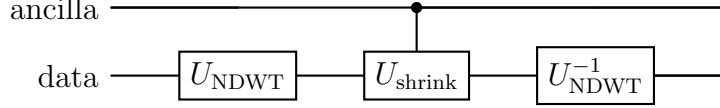


Fig. 6: Coefficientwise shrinkage in the QNDWT domain via an ancilla-driven channel. The data register is mapped into the redundant wavelet domain by U_{NDWT} , interacts with an ancilla (or environment) through a joint unitary whose reduced action implements attenuation U_{shrink} , and is mapped back by U_{NDWT}^{-1} . Measuring the time-domain register yields a denoised signal.

across all shifts and no repeated transform evaluations are required.

Unitary dilation and ancilla controlled attenuation. Attenuation can be implemented as a unitary dilation on a larger Hilbert space. Let $U(\theta)$ denote a parametrized joint unitary acting on the data and an auxiliary environment register. After tracing out the environment, the data experiences a contraction of selected components. For small θ the contraction is smoothly tunable in θ , mirroring classical shrinkage while realizing the effect through reversible evolution followed by coarse graining. For more about wavelet quantum shrinkage see Vidakovic (2025).

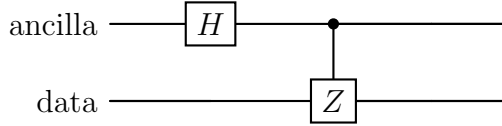


Fig. 7: Ancilla driven dephasing as a primitive for attenuation. Preparing the ancilla in superposition and applying a controlled Z gate induces, after discarding the ancilla, a phase damping channel on the data qubit. Applied coefficientwise in the QNDWT basis, this yields smooth shrinkage of wavelet components.

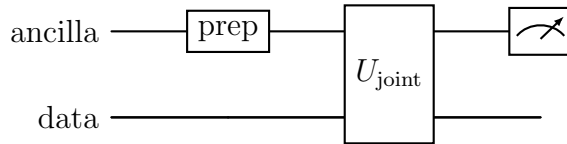


Fig. 8: Stinespring dilation of a CPTP map for QNDWT shrinkage. A joint unitary U_{joint} on ancilla and data induces, after discarding or measuring the ancilla, a Kraus representation that is diagonal or approximately diagonal in the redundant wavelet basis, attenuating small coefficients while preserving dominant structure.

7.2 Energywise processing: Scalograms and multiscale spectra

The Hadamard formulation of Section 5 is designed for tasks that depend on NDWT energies rather than signed coefficients. Instead of constructing the full redundant coefficient array, one queries scale-shift energies or level energies through controlled diagonal unitaries and Hadamard tests. This is particularly useful when only energy summaries

are needed (scalograms, spectra, scaling exponents), or when near-term constraints favor shallow diagonal circuits and measurement-based estimation.

Example 4. NDWT Energy Representation and Log-Spectrum (db2, $N = 512$). This example illustrates the use of NDWT energies for spectral analysis of a turbulent wind-velocity signal (Vidakovic, Katul, & Albertson, 2000). Under Kolmogorov's K41 theory, fully developed turbulence exhibits a power law spectrum consistent with the scaling of fractional Brownian motion with Hurst exponent $H = 1/3$.

Figure 9 shows the turbulent velocity time series U_n , $n = 0, \dots, 511$, sampled at 56 Hz, which serves as the input for subsequent wavelet analysis.

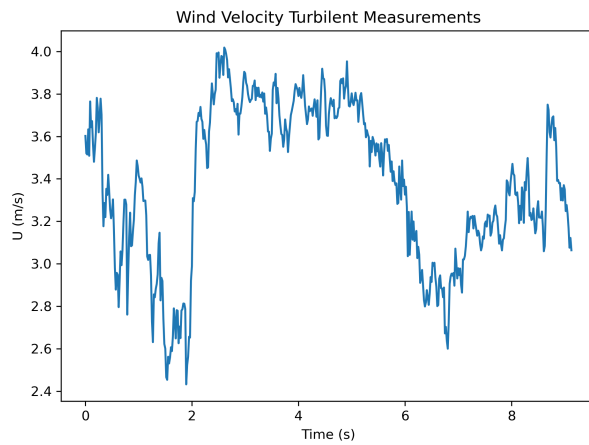


Fig. 9: Turbulent wind-velocity signal U_n of length $N = 512$ (sampling rate 56 Hz).

Figure 10 displays energy summaries from a 7-level NDWT using the Daubechies 2 wavelet. The left panel shows a stacked representation of stationary wavelet energies, with rows ordered as

$$[a_7, d_7, d_6, \dots, d_1],$$

where d_1 denotes the finest and d_7 the coarsest detail level. The right panel shows the corresponding NDWT log-spectrum, constructed from the average scale energies

$$E_j = \frac{1}{N} \sum_{n=0}^{N-1} |d_j[n]|^2, \quad j = 1, \dots, 7. \quad (11)$$

A linear fit of $\log_2 E_j$ versus j provides a slope that, for self-similar models, is interpreted through the relation $\log_2 E_j \approx (2H + 1)j + \text{const}$. This slope in the literature is traditionally reported as negative, but because of our indexing of j s, the slope is positive.

In the quantum setting, Section 4 shows that the reduced density operator $\rho_D = \text{Tr}_A(\rho)$ already averages over the epsilon-decimated shift index. Expectation values of level projectors on ρ_D provide quantum estimates of level energies, and Hadamard tests can be used to evaluate the required overlap quantities without explicitly forming all

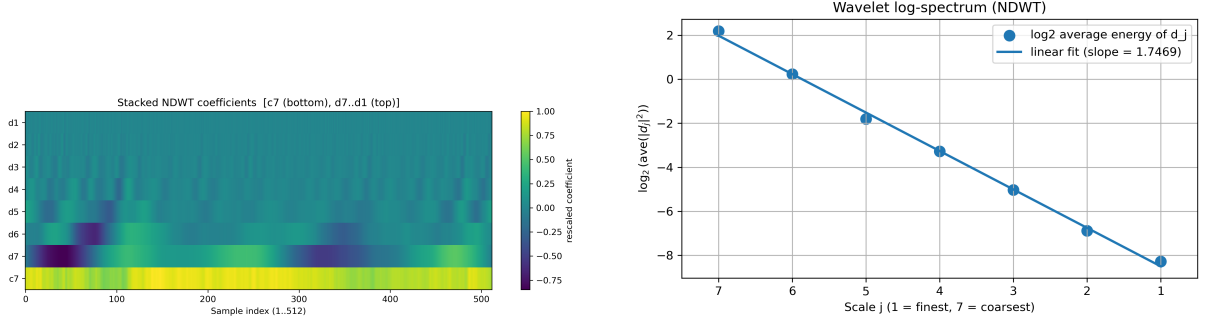


Fig. 10: NDWT energy localization across scale and time (db2, $L = 7$, $N = 512$).

shifted transforms. Repeated queries across j therefore yield a quantum NDWT spectrum, i.e., $\log_2 E_j$ versus j , directly in the energy domain. For fractional Brownian motion indexed by Hurst exponent H , classical NDWT spectra produce slopes near $(2H + 1)$. Because the quantum estimates are naturally shift averaged, the same scaling behavior is expected, potentially with reduced variance due to coherent averaging. This example can be found in the notebook `QNDWT005.ipynb`.

The two application modes above yield translation-invariant multiscale information but emphasize different outputs. The epsilon-decimated formulation provides coefficient access suitable for coherent denoising and attenuation prior to measurement, with shift invariance enforced by uniform treatment across the shift register. The Hadamard formulation provides direct access to energy scalograms and spectra through expectation values, avoiding full coefficient recovery. Together, these uses illustrate how the quantum NDWT supports both coefficientwise processing and energywise multiscale summarization within a unified framework.

8 Conclusion

This paper developed two complementary quantum formulations of the nondecimated wavelet transform and showed how classical translation-invariant multiscale ideas can be embedded coherently into quantum computation. Both constructions are rooted in the epsilon-decimated interpretation of the classical NDWT (Section 2), which expresses the redundant transform as a structured family of orthogonal wavelet analyses indexed by circular shifts.

The first formulation, introduced in Sections 3 and 4, promotes the shift index ε to a quantum register and realizes all shifted wavelet transforms coherently through controlled circular shifts followed by a wavelet analysis unitary. This epsilon-decimated quantum NDWT yields an explicit coefficient-domain representation in which redundancy and shift invariance are preserved by design. Because the entire redundant library is encoded in a single joint state, subsequent processing—such as attenuation, shrinkage,

or feature extraction—can be carried out coherently before measurement. As discussed in Sections 4 and 7, ancilla–driven completely positive trace preserving maps provide a physically meaningful mechanism for quantum shrinkage, allowing nonlinear denoising effects to be realized without violating unitarity.

The second formulation, developed in Section 5, uses the Hadamard test to access non-decimated wavelet information through expectation values of diagonal phase operators. Rather than producing signed coefficients, this approach yields shift–invariant energy scalograms and multiscale spectra directly in the energy domain. Redundancy arises through systematic probing over scale–shift pairs, while unitarity is preserved throughout. This formulation is particularly well suited for near–term quantum devices, where shallow diagonal circuits and overlap estimation are more practical than deep multiplexed unitaries, and where the primary goal is spectral or scaling analysis rather than coefficientwise reconstruction.

Although operationally distinct, the two constructions address complementary aspects of translation–invariant wavelet analysis. The epsilon–decimated formulation provides coefficient–level access and supports coherent postprocessing, while the Hadamard formulation provides direct access to quadratic summaries and invariant features. Both exploit quantum parallelism to replace the classical enumeration of shifts, and both naturally accommodate measurement strategies that emphasize robustness and variance reduction. Together, they establish a flexible framework in which redundancy, coherence, and measurement cost can be balanced according to hardware constraints and application requirements.

Several directions for future work emerge from this framework. On the algorithmic side, optimized compilation of redundant wavelet unitaries and hybrid schemes that combine epsilon–decimated state preparation with Hadamard–test readout merit further study. From a statistical perspective, quantum Bayesian shrinkage and adaptive attenuation strategies based on redundant coefficient statistics offer a promising extension of classical wavelet methodology. More broadly, continuous and overcomplete wavelet transforms, multichannel and multidimensional signals, and data–driven or adaptive wavelet constructions provide natural avenues for extending the present theory.

Overall, the results presented here demonstrate that nondecimated wavelet ideas are not only compatible with quantum computation, but in many respects naturally aligned with it. By unifying redundancy, shift invariance, and multiresolution structure within coherent quantum architectures, the quantum NDWT provides a principled foundation for multiscale analysis, denoising, and inference on emerging quantum platforms.

Acknowledgments. The author gratefully acknowledges support from the National Science Foundation under Grant No. 2515246 at Texas A&M University and from the H. O. Hartley Chair research funds at Texas A&M. The author also thanks Nick Broon

of IBM Quantum for valuable discussions during his visit to Texas A&M.

References

Abraham, H., Akhalwaya, A., Banerjee, T., Baiardi, A., et al. (2023). *Qiskit: An open-source framework for quantum computing*. <https://qiskit.org/>.

Aharonov, D., Jones, V., & Landau, Z. (2009). A polynomial quantum algorithm for approximating the jones polynomial. In *Algorithmica* (Vol. 55, pp. 395–421). Springer.

Bagherimehrab, M., & Aspuru-Guzik, A. (2023). Efficient quantum algorithm for all quantum wavelet transforms. *Quantum*, 7, 1103. doi: 10.22331/q-2023-10-10-1103

Fijany, A., & Williams, C. P. (1998a). Quantum wavelet transforms and their implementation. In C. P. Williams (Ed.), *Quantum computing and quantum communications* (Vol. 1509, pp. 10–33). Berlin, Heidelberg: Springer. doi: 10.1007/BFb0053328

Fijany, A., & Williams, C. P. (1998b). Quantum wavelet transforms: Fast algorithms and complete circuits. In *Proceedings of the spie conference on quantum computing* (Vol. 3076, pp. 175–183). doi: 10.1117/12.302230

Holschneider, M., Kronland-Martinet, R., Morlet, J., & Tchamitchian, P. (1989). A real-time algorithm for signal analysis with the help of the wavelet transform. In *Wavelets: Time-frequency methods and phase space* (pp. 286–297). Springer.

Klappenecker, A. (1999). Wavelets and wavelet packets on quantum computers. In *Proceedings of the 3rd international conference on computational intelligence and multimedia applications (iccima)* (pp. 169–173). IEEE. doi: 10.1109/ICCIMA.1999.795210

Li, H.-S., et al. (2019). Quantum wavelet transforms for general orthogonal wavelets. *Quantum Information Processing*, 18(2), 50. doi: 10.1007/s11128-018-2042-3

Li, Z. H., Li, J., Li, F. G., & Xu, S. J. (2018). The multi-level and multi-dimensional quantum wavelet transform. *Quantum Information Processing*, 17(9), 240. doi: 10.1007/s11128-018-2000-y

Nason, G. P., & Silverman, B. W. (1995). The stationary wavelet transform and some statistical applications. In A. Antoniadis & G. Oppenheim (Eds.), *Wavelets and statistics* (Vol. 103, pp. 281–300). New York: Springer. doi: 10.1007/978-1-4612-2544-7_17

Percival, D. B., & Walden, A. T. (2000). *Wavelet methods for time series analysis*. Cambridge University Press.

Podzorova, N. (2025). Quantum wave atom transforms. *Quantum Information Processing*. (In press)

Shensa, M. J. (1992). The discrete wavelet transform: Wedding the a trous and mallat algorithms. *IEEE Transactions on Signal Processing*, 40(10), 2464–2482. doi:

10.1109/78.157290

Starck, J.-L., & Murtagh, F. (1994). Image restoration with the a trous algorithm. *Astronomy and Astrophysics*, 288, 342–350.

Vidakovic, B. (1999). *Statistical modeling by wavelets*. Wiley.

Vidakovic, B. (2025, November). *Quantum Framework for Wavelet Shrinkage*. Retrieved from <https://arxiv.org/abs/2511.19855> (arXiv preprint)

Vidakovic, B., Katul, G., & Albertson, J. (2000). Multiscale denoising of self-similar processes. *Journal of Geophysical Research: Atmospheres*, 105(D22), 27049–27058. doi: 10.1029/2000JD900479